

MRTF-A-mediated protection against amyloid- β -induced neuronal injury correlates with restoring autophagy via miR-1273g-3p/mTOR axis in Alzheimer models

Wei Zhang¹, Yuewang Yang², Zifei Xiang³, Jinping Cheng¹, Zhijun Yu³, Wen Wang¹, Ling Hu³, Fuyun Ma², Youping Deng⁴, Zhigang Jin¹, Xiamin Hu²

¹Affiliated Wuhan Resources and Wisco General Hospital, Wuhan University of Science and Technology, Wuhan, Hubei, China

²College of Pharmacy, Shanghai University of Medicine and Health Sciences, Shanghai, China

³College of Medicine, Wuhan University of Science and Technology, Wuhan, Hubei, China

⁴Bioinformatics Core Department of Quantitative Health Sciences, John A. Burns School of Medicine, University of Hawaii, Honolulu, HI 96813, USA

Correspondence to: Xiamin Hu, Zhigang Jin; **email:** huxm@sumhs.edu.cn, jinzhang@crmedical.hk

Keywords: Alzheimer disease, autophagy, miR-1273g-3p, MRTF-A, mTOR

Received: March 22, 2021

Accepted: December 7, 2021

Published: May 23, 2022

Copyright: © 2022 Zhang et al. This is an open access article distributed under the terms of the [Creative Commons Attribution License](https://creativecommons.org/licenses/by/3.0/) (CC BY 3.0), which permits unrestricted use, distribution, and reproduction in any medium, provided the original author and source are credited.

ABSTRACT

Myocardia-Related Transcription Factors-A (MRTF-A), which is enriched in the hippocampus and cerebral cortex, has been shown to have a protective function against ischemia hypoxia-induced neuronal apoptosis. However, the function of MRTF-A on β -amyloid peptide ($A\beta$)-induced neurotoxicity and autophagy dysfunction in Alzheimer's disease is still unclear. This study shows that the expression of MRTF-A in the hippocampus of Tg2576 transgenic mice is reduced, and the overexpression of MRTF-A mediated by lentiviral vectors carrying MRTF-A significantly reduces the accumulation of hippocampal β -amyloid peptide and reduces cognition defect. Overexpression of MRTF-A inhibits neuronal apoptosis, increases the protein levels of microtubule-associated protein 1 light chain 3-II (MAP1LC3/LC3-II) and Beclin1, reduces the accumulation of SQSTM1/p62 protein, and promotes autophagosomes-Lysosomal fusion *in vivo* and *in vitro*. Microarray analysis and bioinformatics analysis show that MRTF-A reverses $A\beta$ -induced autophagy impairment by up-regulating miR-1273g-3p level leading to negative regulation of the mammalian target of rapamycin (mTOR), which is confirmed in $A\beta_{1-42}$ -treated SH-SY5Y cells. Further, overexpression of MRTF-A reduces $A\beta_{1-42}$ -induced neuronal apoptosis. And the effect was abolished by miR-1273g-3p inhibitor or MHY1485 (mTOR agonist), indicating that the protection of MRTF-A on neuronal damage is through targeting miR-1273g-3p/mTOR axis. Targeting this signaling may be a promising approach to protect against $A\beta$ -induced neuronal injury.

INTRODUCTION

Alzheimer's disease is a common progressive neurodegenerative disorder characterized by cognitive dysfunction. The pathological features of Alzheimer's disease include senile plaques composed of amyloid-beta and neurofibrillary tangles, accompanied by the loss of

neurons and synapses in the brain and the proliferation of glial cells [1]. Although its etiology is unknown, assumptions of pathogenesis are proposed, such as β -amyloid peptide accumulation, neurons apoptosis, genetic mutations, synaptic dysfunction, etc. [2–5]. The brains of AD patients display considerable, pathological β -amyloid peptide and presenilin1 protein [6, 7].

The myocardin and myocardin-related transcription factors (MRTF-A and -B), as a co-activator of serum response factor (SRF), synergistically activates the transcription of a subset of genes involved in cytoskeletal organization and muscle cell differentiation [8]. MRTF-A gene expression is enriched in forebrain, especially in hippocampus and cerebral cortex [9, 10], which plays an important role of normal brain development. MRTF-A mutant mice exhibited abnormal neuronal migration and impaired neurite outgrowth, as well as decreased expression and activity of actin and actin-severing proteins gelsolin and cofilin [11]. Our previous study has shown that MRTF-A attenuates hydrogen peroxide-induced and A β -induced neuronal injury in primary cortical neuron by upregulating Bcl-2 and Mcl-1 through triggering their CARG box [12, 13]. However, the role of MRTF-A in the regulation of AD progression has not been systematically illustrated. Based on the miRNA microarray analysis, we found that miR-1273g-3p might involve in the protection of MRTF-A on A β -induced neuronal injury. However, whether MRTF-A affect the AD progression via regulating miR-1273g-3p is unknown.

MicroRNA represents an evolutionarily conserved 20-23 nucleotide group [14]. Studies have shown that some miRNAs seem to be involved in the AD process, which create highly complex and interactive regulatory miRNA-mRNA networks in an independent, coordinated and/or cooperative manner inducing to changes in atypical mRNA abundance, gene expression, pro-inflammatory signals, synapses, and amyloidosis [14–16]. The main mode of miRNA action is to recognize the 3' untranslated region (3'-UTR) of a specific messenger RNA (mRNA) target through base pair complementation [14]. Using the bioinformatic analysis, we found a Homo sapiens (Hsa) miR-1273g-3p binding site exists in the 3'-UTR of the mammalian target of rapamycin (mTOR), predicting that miR-1273g-3p might negatively regulate mTOR expression.

mTOR is a conserved serine/threonine protein kinase, which belongs to the phosphoinositide-3-kinase (PI3K)-related kinase family of protein kinases [17]. Some small molecules, including small non-coding RNA (sncRNA) molecules, can regulate autophagy through mTOR-dependent or independent pathways [18, 19], and are shown a protective effect in neurodegenerative disease models [20, 21], suggesting the mTOR pathway is one of the most promising targets for AD treatment via regulating autophagy [22]. Therefore, we speculated that mTOR may be involved in the effect of MRTF-A on A β -induced neuronal injury via miRNA-mRNA interaction with miR-1273g-3p.

This study was to investigate the effect of MRTF-A on A β -induced neurotoxicity in the models of Tg2576 AD mouse and A β ₁₋₄₂-treated SH-SY5Y cell. According to the hypothesis of MRTF-A regulating miR-1273g-3p/mTOR axis, we further investigated the mechanism of MRTF-A based on bioinformatics analysis and experimental verification. Our results might provide new avenues for therapeutic approaches of AD.

MATERIALS AND METHODS

Construction of lentivirus carrying MRTF-A and microinjection

To investigate the effect of MRTF-A on Tg2576 mice, the GV287 lentivirus (GOSL29806, Genechem Co., Ltd.) mediating MRTF-A overexpression (LV-MRTF-A) was constructed. Mouse MRTF-A cDNA (NM001082536) was amplified by PCR: MRTF-A Forwards: GAGGATCCCCGGGTACCGGTCGCCACCATGCCGCCTTTGAAAAGCCCCGCTG; MRTF-A Reverse: TCCTTG TAGTCCATACCCAAGCAGGAATCCCAGTGGAGCTGC). Subsequently, insert the PCR product into the parent vector Ubi-MCS-3FLAG-SV40-EGFP (Genechem Co., Ltd, China) between the Age I and BamH I sites, and empty as negative control (LV-NEG) [23]. The lentivirus was produced by co-transfected with a transfer vector and three packaging vectors (pGC-LV vector 20 μ g, pHelper-1.0 vector 15 μ g, pHelper-2.0 vector 10 μ g), and then purified by ultracentrifugation, and its titer was determined via fluorescence.

Using a microinjection system, mice is anesthetized and placed in a stereotactic device (Zhenghua biological instrument equipment co., LTD), afterward the mice were bilateral injected with 4.0 μ L of purified virus into the lateral ventricle (-2.5 mm dorsal/ventral, -1.0 mm lateral, and -0.22 mm anterior/posterior to bregma) [24]. The transfection efficiency *in vivo* was measured by western blot analysis after one month of injection.

Animals and treatment

Tg2576 mice carrying human APP695 with Swedish double mutations (hAPP; HuAPP695; K670N/M671L) were gifted by Dr. Zeng Yan (Wuhan University of Science and Technology, China). Wild-type male C57BL mice (Certificate No: SCXK (Q)2015-0018) were purchased from the Hubei Provincial Center for Disease Control and Prevention. All mice were allowed free access to food and water before the procedure was performed under optimal conditions (12/12 hours light/dark with humidity at 60 \pm 5% and temperature at 22 \pm 3 $^{\circ}$ C) [25].

Mice (about 6.5 months old) were randomly divided into 3 groups: (i) Tg2576 mice microinjected with LV-MRTF-A (n=14); (ii) Tg2576 mice microinjected with LV-NEG (n=14); (iii) Age-matched C57BL/6 (WT) mice microinjected with normal saline (n=12). Microinjection of LV-MRTF-A, LV-NEG or normal saline were treated once every 2 weeks for 6 weeks, including 2 weeks of behavioral test [26]. The experimental arrangement is summarized in Figure 1B. After behavioral evaluations, the mice were sacrificed and the brains were taken off for the analysis of western blot, immunohistochemical, Nissl staining and transmission electron microscope.

Behavioral test

The behavioral test was performed as described previously. Morris water maze (MWM) test was carried out in a circular plastic pool filled with opaque water of skimmed milk kept at $25 \pm 1^\circ$ C. The escape platform was submerged 1-1.5cm below the water surface. The time spent by each mouse to locate the platform (escape latency) and its track were recorded by a camera (Panlab, Barcelona, Spain). After 24 hours of MWM test, a memory test (probe test) was performed by removing the platform. The mice were allowed to swim freely for 60 s. The retention ability of memory was estimated by the time spent in the target quadrant area [27].

Passive avoidance performance test was performed in two compartments (light and dark compartments) (Med Associates Inc., Vermont, USA) [26]. At the beginning, the mice were placed in an illuminated compartment for training. And then the mice were moved into the dark compartment and received an electric shock. Then the mice were returned to their cage. One day later, the mice were placed in the illuminated compartment, and the latency to enter the dark compartment was measured, described as step-through latency.

Nissl staining

After neurobehavioral evaluation, mice (3 animals/group) were anesthetized, and then the brain was removed. The paraffin-embedded mouse hippocampus was cut into 4 mm thick sections. After deparaffinization and rehydration, the sections were stained in Nissl staining solution at 60° C for 30 minutes (C0117, Beyotime Biotechnology, Shanghai, China). The sections are dehydrated with absolute ethanol, xylene is transparent and sealed with neutral gum. The morphology was observed using a multifunctional digital pathology system (APERIO VERSA 8, Leica, Germany).

Transmission electron microscope analysis

Autophagic vacuoles were assessed by electron microscopy. After heart perfusion with glutaraldehyde, hippocampal CA1 area was separated and fixed in 4 % paraformaldehyde for 2 hours then embedded with epoxy resin. The samples were sliced into 90 nm ultrathin sections and observed under HZ600 transmission electron microscope (Hitachi, Japan).

Immunofluorescence staining

The immunofluorescence staining of brain paraffin sections were performed as previously described [25]. After blocking with 5% bovine serum albumin, the sections were incubated with anti-MRTF-A (1:100, sc-398675, Santa Cruz, CA, USA), rabbit anti- β -amyloid (Cell Signaling Technology, 1:2000) or rabbit anti-LC3B (1: 500, ab48394, Abcam, MA, USA), respectively. Then, the sections were washed with 0.1M PBS and then incubated with the fluorescence-labeled secondary antibodies (goat anti-mouse/rabbit 1:200, ab150113, ab150077, Abcam, MA, USA) for 30 minutes at 37° C, and then washed with PBS. Next, the nuclei were stained with DAPI (5 μ g/ml) for 2 minutes, and then analyzed with a laser scanning confocal microscope (CX31-32RFL, Olympus).

Cell culture and treatment

Human SH-SY5Y cells were grown in DMEM high glucose with 10% fetal bovine serum (G4510, Servicebio, Shanghai, China) and 1% penicillin-streptomycin solution at 37° C in a humidified incubator containing 5% CO_2 . For the effect of MRTF-A on $\text{A}\beta_{1-42}$ -induced SH-SY5Y cell damage, the cells were firstly transduced with or without LV-MRTF-A (Genechem, Shanghai, China), miR-1273g-3p mimics (Sequence: 5'-ACCACUGCACUCCAGCCUGAG-3'), miR-1273g-3p inhibitors (Sequence: 5'-CUCAGGCUGGAGUGCAGUGGU-3') and their negative (Ribobio, Guangzhou, China) as control. After 48 hours, the cells were exposed to $\text{A}\beta_{1-42}$ (#89298, 10 μ M, GL Biochem, Shanghai, China) for 24 hours. In addition, to prove the effect of mTOR involved in MRTF-A against $\text{A}\beta$ -induced neuronal damage, MHY1485(5 mM) (an agonist of mTOR; S7811, Selleck, Shanghai, China) and 3-Methyladenine (5 mM) (3-MA; S2767, Selleck, Shanghai, China) were also used to co-incubate in the cells for 24 hours, and then exposed to 10 μ M $\text{A}\beta_{1-42}$.

Cell viability assay

SH-SY5Y cells were seeded into 96-well plates at a density of 8×10^3 cells per well. Transfection of LV-MRTF-A or its negative control for 48 hours, and then

incubated with or without 10 μ M of A β ₁₋₄₂ at 37° C for 24 hours. 20 μ L of 3-(4,5-dimethylthiazole-2-yl)-2,5-diphenyl tetrazolium bromide (5 mg/mL, M2128, Sigma-Aldrich St. Louis, USA) was added to each well for 4 hours at 37° C in darkness. After removing the supernatant, 150 μ L of dimethyl sulfoxide was added to dissolve the crystalline formazan. The absorbance was measured using a microplate reader at 490 nm (Synergy 4, Omega Bio-tek, Inc., Norcross, GA, USA).

TUNEL labeling

The cultured cells were labeled with the TUNEL Bright Red Apoptosis Detection Kit System (A113-01/02/03, Vazyme Biotech, China). Specimens were viewed on a CX31-32RFL confocal microscope. The cells undergoing apoptosis and the total number of cells were measured (Image J software). The apoptotic ratio was apoptotic cells/total cells 100% [28].

Real-time RT-PCR analysis

miR-1273g-3p expression was determined using the Bulge-Loop miRNA qRT-PCR Primer Set (MQPS 0002237-1-100, RiboBio, China) [29]. Amplification was carried out starting with an initial step of 3 min at 95° C, followed by 40 cycles of the amplification step for miR-1273g-3p and U6(MQPS0000002-1-100). The primer sequences were synthesized by Ribobio technology Company (Guangzhou, China).

Western blotting analyses

The protein expressions of the brain tissues and cell specimens were analyzed as described previously [25]. The primary antibodies included MRTF-A (1:1000, sc-398675, Santa Cruz, CA, USA), APP (#2452, Cell Signaling Technology, MA, USA), and BACE1 (1:1000, sc-33711, Santa Cruz, CA, USA), p62(1:1000, P0067, Sigma-Aldrich St. Louis, USA), Beclin1(1:1000, #3738, Cell Signaling Technology, MA, USA), mTOR (1:1000, ab32028, Abcam, MA, USA), p-mTOR(1:1000, sc-293133, Santa Cruz, CA, USA), and β -actin (1:1000, sc-8432, Santa Cruz, CA, USA). The antibodies were diluted in TBST buffer (50mM TrisHCl, 150mM NaCl, 0.1% Tween-20, pH 7.4) (P0015F, Beyotime, Shanghai, China) and incubated with the PVDF membrane at 4° C overnight. Corresponding horseradish peroxidase (HRP)-conjugated secondary antibodies (1:5000, sc-2004, sc-2005, Santa Cruz, CA, USA) was subsequently incubated with the PVDF membrane for 90 minutes at room temperature. Signal detection was performed with an enhanced chemiluminescent (ECL) reagent (G2020-25ML, Servicbio, Shanghai, China). The luminescent signals were detected by a BioRad ChemiDoc MP system.

Autophagic flux measurement

Cells were cultured in 24-well plates (1 \times 10⁵ cells/well), and then were transfected with the adenovirus of mCherry-GFP-LC3 (20 MOI, multiplicity of infection) at 37° C in 5%CO₂/95% air. After 24 hours for infection, removed the virus-containing culture medium and then transduced with or without LV-MRTF-A, miR-1273g-3p mimics, miR-1273g-3p inhibitors or their negative, and then exposed to A β ₁₋₄₂ for 48 hours. The expression of mCherry and GFP was visualized with confocal laser scanning microscopy (Olympus) [30]. The dots of GFP and mCherry were measured in 3 randomly selected areas under fluorescence microscope (Olympus Corporation).

miRNA microarray

Cells were transduced with or without LV-MRTF-A for 48 hours and then incubated with 10 μ M A β ₁₋₄₂. 24 hours later, total RNA was extracted from cells of each group using Trizol reagent (#15596-026, Invitrogen, Carlsbad, CA, USA). RNA quality was measured using Agilent 2100 Bioanalyzer (Agilent Technologies). Only an RNA integrity number \geq 5 was used for further analyses. The coefficient variance (CV) of repeated probe was calculated. The next microarray analysis uses the invariant set normalization method. The miRNAs with expression differences of more than 2.0 times were considered to be significant gene.

Dual luciferase reporter assay

mTOR cDNA (position 500-800bp) containing mir-1273g-3p predictive binding site of mTOR 3'-UTR (position 684-690) was cloned into pmirGLO dual luciferase miRNA target expression vector (Promega Corporation, Fitchburg, WI, USA) to construct the report vector pmirGLO-mTOR-wt (wild-type). The mutant mTOR, containing a point mutation at the binding site of mir-1273G-3p seed region, was inserted into the vector pmirGLO-mTOR-mut (mutant). Transfection of 293T line with miR-1273g-3p mimics or scramble control, or co-transfected with 10 μ g of pmir-GLO-wt-mTOR or pmir-GLO-mTOR-mut using Lipofectamine 3000 transfection reagent (L3000015, Thermo Fisher Scientific). 48 hours later, cells were collected and lysed. Then the luciferase activities were determined using Dual-Luciferase® Reporter Assay System (E1910, Promega Corporation).

Statistical analysis

Data are presented as means \pm SEM. Statistical analyses were carried out with SPSS 16.0. A *P* value less than 0.05 was considered to be statistically significant.

Differences among ≥ 3 groups were statistically analyzed by One-way analysis of variance (ANOVA) followed by Tukey's post hoc test.

RESULTS

Upregulating MRTF-A ameliorated cognitive deficits in Tg2576 mice

Tg2576 mice develop cognitive impairment at about 6-12 months of age [31, 32], was used to explore the role of MRTF-A on cognitive impairments. Data showed that MRTF-A endogenous expression in hippocampus of Tg2576 mouse was decreased significantly compared to wild-type (WT) mice (Figure 1A). To verify overexpression of MRTF-A improved cognitive deficit in Tg2576 mice, mice were preinjected with either MRTF-A lentivirus (LV-MRTF-A) or negative control lentivirus (LV-NEG) into their lateral ventricles once every 15 days. Markedly increasing of MRTF-A expression was observed in Tg2576 mice treated with LV-MRTF-A compared with LV-NEG group at 7 and 14 days after injection (Figure 1A). The behavior tests were performed to assess the spatial ability of learning and memory according to the experiment schedule (Figure 1B). Compared with Tg2576 mice alone or Tg2576 mice treated with negative control lentivirus (LV-NEG), overexpression of MRTF-A reduced the average escape latency and swimming distance of Tg2576 mice, especially at the day 5 or 6 (Figure 1C, 1D). Transfection of LV-MRTF-A prolonged the time in the target quadrants significantly in LV-MRTF-A - treated mice compared to that in Tg2576 mice or in Tg2576+LV-NEG mice. Passive avoidance test is performed on the second day after the probe test. There was no significant difference between Tg2576 mice and Tg2576+LV-NEG mice. The average step latency of Tg2576+LV-NEG mice in the illuminated compartment was 59.70 ± 15.31 seconds, while the average step latency of LV-MRTF-A treated mice was 128.7 ± 28.50 seconds, which was significantly higher than that of the control group (Figure 1F). These results indicate that MRTF-A may be involved in the pathogenesis and development of AD in mice.

Overexpression of MRTF-A reduced A β -induced neurotoxicity in Tg2576 mice

The level of insoluble A β in the brain of Tg2576 mice increased significantly at about 6 months of age, accumulating into A β plaques at 7-8 months of age [33]. Upregulating MRTF-A significantly decreased the A β plaque burden (Figure 2A) and the expression of APP and BACE1 compared with Tg2576+LV-NEG group (Figure 2B, 2C). Next, we explored whether MRTF-A reduces A β -induced neurotoxicity. Nissl staining

showed that compared with WT mice, Nissl body loss, neuron atrophy and nuclear contraction occurred in the hippocampal CA area of Tg2576+LV-NEG mice, accompanied by neuron reduction (Figure 2D, 2E). However, by overexpression of MRTF-A, this morphological change and neuron loss can be reduced (Figure 2D, 2E).

Overexpression of MRTF-A rescued A β -induced autophagy deficit in Tg2576 mice

Autophagy plays a crucial role in maintaining intracellular homeostasis, which is considered a pro-survival mechanism against stimuli that trigger apoptosis [34, 35]. A defect in autophagosome maturation at the stage of autophagosome-lysosome fusion is an important feature of AD pathology and cognitive dysfunction [36, 37], suggesting a protective role of autophagy against neurodegeneration [38]. Through the construction of co-expression network and node degree analysis, we found that there were some functional and highly connected hubs in MRTF-A, such as ATG5, Beclin1 and so on (Supplementary Figure 1), predicting MRTF-A as an autophagy regulator. MAP1LC3/LC3 is a key regulator of autophagy, which participates in several steps [39]. LC3-II interacts with p62 bodies and thereby facilitate the elongation and closure of autophagosomal membrane [40]. Here, we found that compared with Tg2576 or Tg2576+LV-NEG group, overexpression of MRTF-A significantly increased LC3B fluorescence intensity (Figure 3A, 3B) and Beclin1 protein level, and reduced the expression of p62 protein in hippocampal region (Figure 3C, 3D). Transmission electron microscopy images showed that autophagosomes were rarely noticed in WT mice, while autophagic vacuoles accumulated abnormally in Tg2576 mice and did not fuse with lysosomes. However, overexpression of MRTF-A resulted in an increase in autophagosomes bound to lysosomes, thereby forming autophagolysosomes (Figure 3E), indicating the reversal effect of overexpression of MRTF-A on autophagy defects.

MRTF-A attenuated A β -induced neurotoxicity through regulating autophagy *in vitro*

The SH-SY5Y cell model treated with A β is used to further study the potential neuroprotective effects and mechanisms of MRTF-A. Cells were transfected with LV-MRTF-A or LV-NEG for 48 hours, and then treated with A β_{1-42} for 24 hours. Compared with LV-NEG transfected cells, MRTF-A protein expression was confirmed to be significantly increased 48 hours after transfection with LV-MRTF-A (Supplementary Figure 2). To identify whether MRTF-A is responsible for rescuing the impairment of A β -induced autophagy flux,

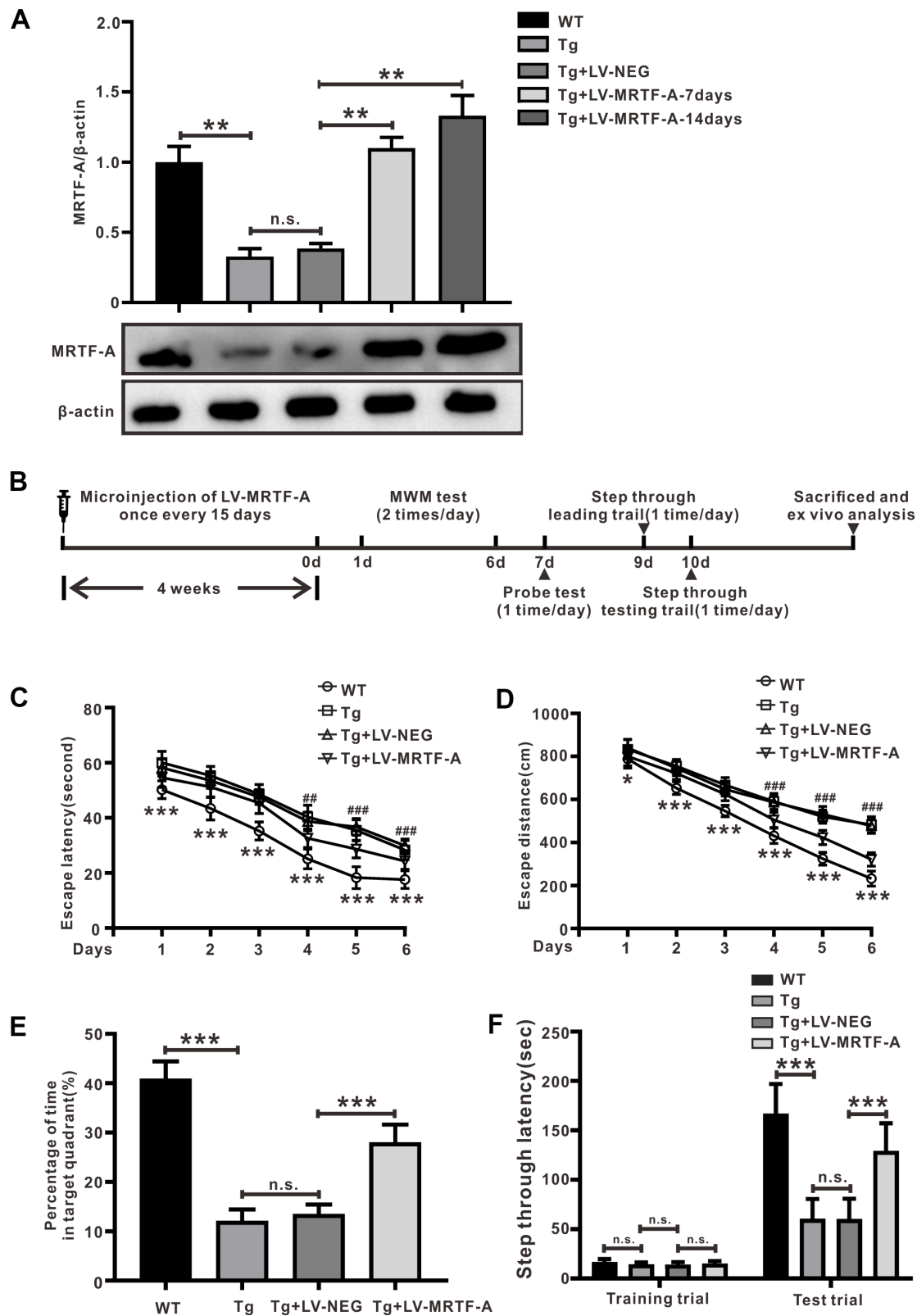


Figure 1. MRTF-A alleviated cognitive impairment in Tg2576 mice. (A) MRTF-A expression in the hippocampus of WT and Tg2576 mice was analyzed after transfected with or without LV-MRTF-A. Data represent means \pm SEM from 5 mice per group. (B) The diagram of the treatment of LV-MRTF-A and the assessment of cognitive function in Tg2576 mice. (C–F) The water maze test (C, D), the probe test (E) and the step-through type passive avoidance test (F) were carried out in WT or Tg2576 mice. Data represent means \pm SEM from 14–12 mice per group, * P < 0.05, ** P < 0.01 and *** P < 0.001 (two-way ANOVA, Tukey’s Multiple Comparison Test).

the changes of APs and ALs were analyzed by confocal microscopy. As known, the yellow spots in the image (GFP and RFP fluorescence co-location) represent APs, while the red spots alone represent ALs. As shown in Figure 4A, 4B, compared with the control group, the yellow and green dots (indicating AP) in the A β or A β +LV-NEG group were increased significantly, while the red dots (indicating AL) did not increase correspondingly. However, transfection of LV-MRTF-

A increased the intensity of red dots in the A β +LV-MRTF-A group (Figure 4A, 4B). Consistent with the above results, compared with the A β +LV-NEG group, transfection of LV-MRTF-A significantly increased Beclin1 level and decreased SQSTM1/p62 level in A β -treated SH-SY5Y cells (Figure 4C, 4D). These results indicate that overexpression of MRTF-A can rescue the impairment of autophagy induced by A β ₁₋₄₂ in SH-SY5Y cells.

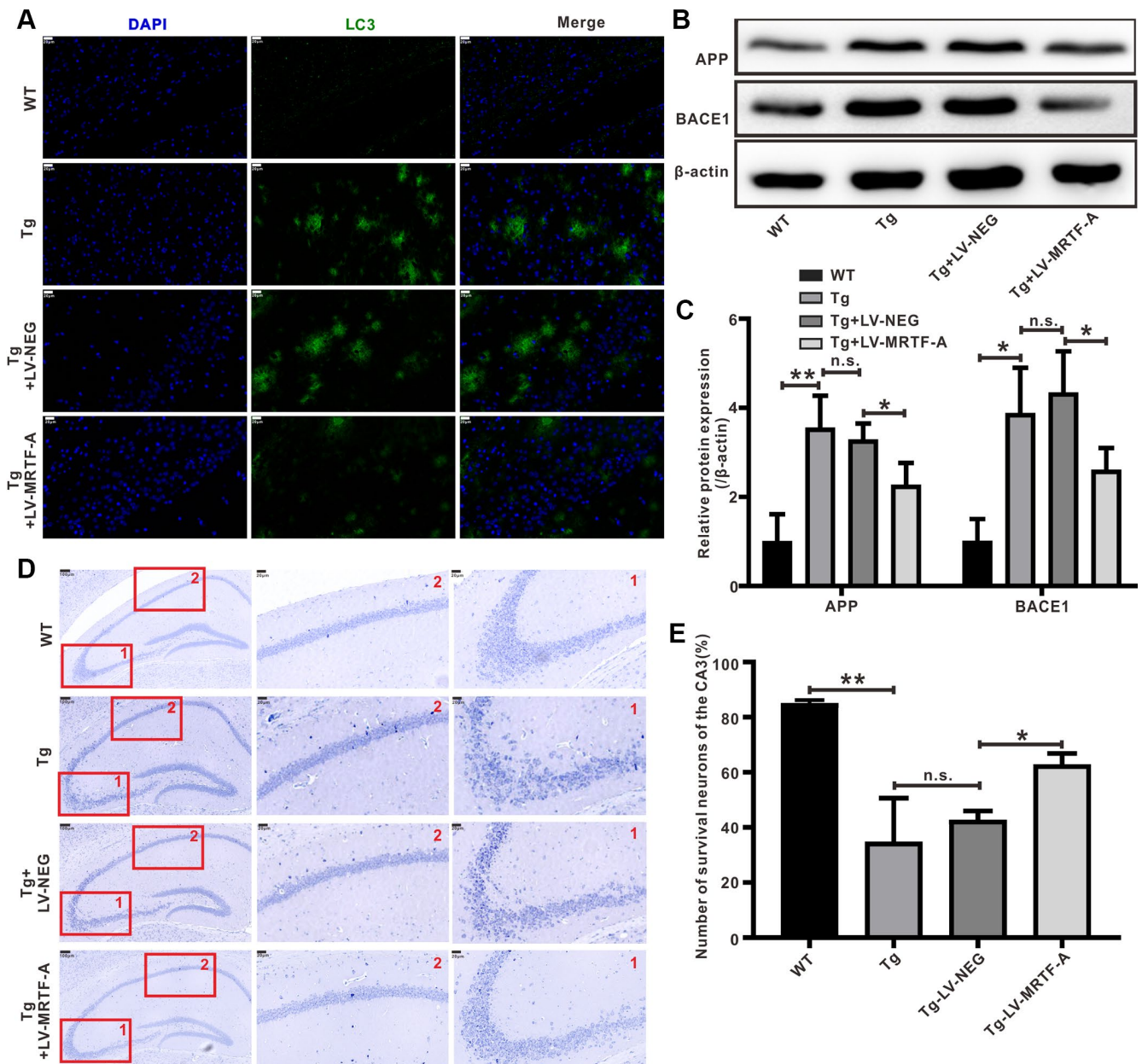


Figure 2. MRTF-A reduced A β -induced neurotoxicity in Tg2576 mouse hippocampus. (A) Representative image of staining with anti-A β (green) and DAPI (blue) in the CA1 areas of Tg2576 mice treated with LV-MRTF-A or not. (B, C) Western blot and quantitative analysis for APP and BACE1 genes. Data are presented as mean \pm SEM from 5 mice per group, * P < 0.05 (one-way ANOVA, Tukey's Multiple Comparison Test). (D, E) Nissl staining for the neuron morphological changes. The number of survival neurons of CA3 areas was analysis. Data represent means \pm SEM from 5 mice per group, * P < 0.05, ** P < 0.01 and *** P < 0.001 (one-way ANOVA, Tukey's Multiple Comparison Test).

In order to further confirm whether the regulation of autophagy by MRTF-A is responsible for its inhibition of neuronal apoptosis, the cells were incubated with 3-MA (Class III PI3K inhibitor) as an autophagy inhibitor. Then cell apoptosis rates were detected by

TUNEL labeling. Compared with the control group, the number of apoptotic neurons in the A β or A β +LV-NEG group was significantly increased. However, compared with the A β +LV-NEG group, the amount of apoptosis in the A β +LV-MRTF-A group was significantly

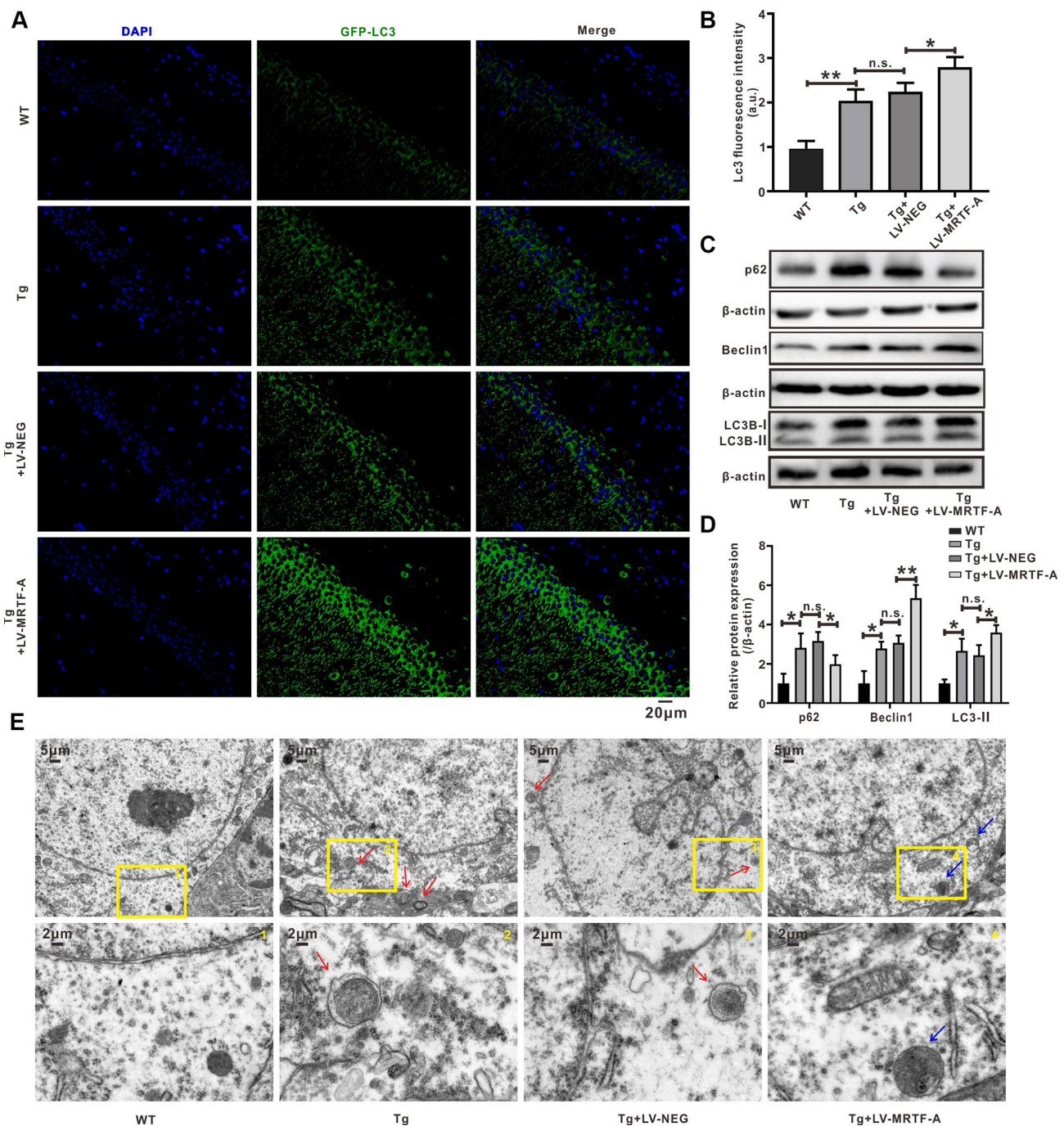


Figure 3. MRTF-A rescued autophagy deficit in Tg2576 mice. (A–D) Immunofluorescence staining and quantitative analysis for LC3B (A, B); simultaneously western blot and quantitative analysis for Beclin1 and SQSTM1/p62 protein expressions (C, D). Data represent means \pm SEM from 3 mice per group, * P < 0.05, ** P < 0.01 and *** P < 0.001 (one-way ANOVA, Tukey's Multiple Comparison Test). (E) Representative transmission electron microscopic images in the hippocampus. Red arrows depict autophagolysosomes and blue arrows depict autolysosomes.

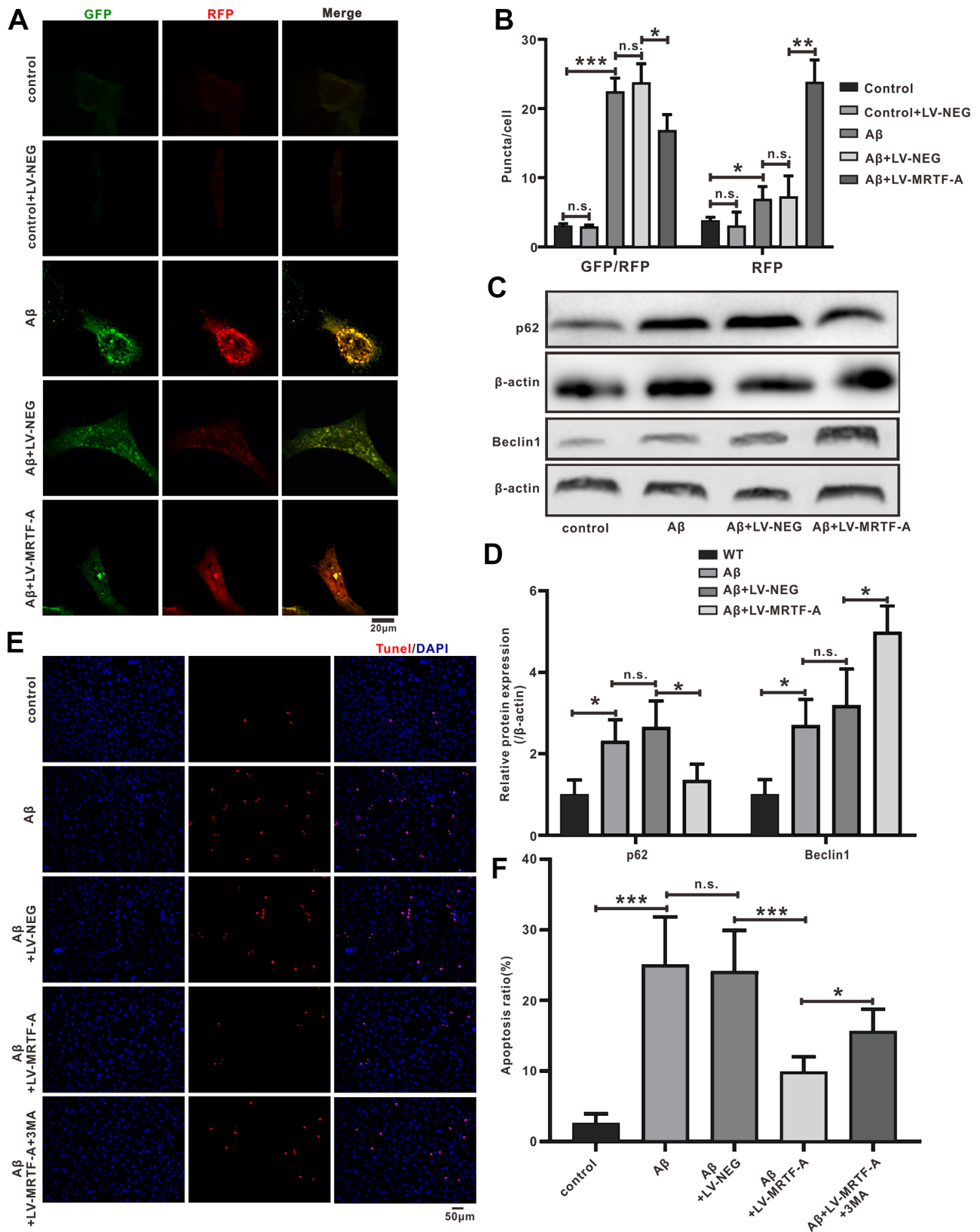


Figure 4. MRTF-A attenuated A β -induced neurotoxicity by promoting autophagy in SH-SY5Y cells. (A, B) The autophagy flux analysis using Ad-mCherry-GFP-LC3B-tagged protein. (C, D) Western blot analysis protein for Beclin1 and p62 expression. (E, F) TUNEL staining for cell apoptosis in A β -treated SH-SY5Y cells followed MRTF-A treatment co-incubation with or without 3-MA. Data represent means \pm SEM of 3 independent experiments. * P < 0.05, ** P < 0.01 and *** P < 0.001 (one-way ANOVA, Tukey's Multiple Comparison Test).

reduced. Further, its inhibitory effect was significantly eliminated by co-incubation with 3-MA (Figure 4E, 4F). These results indicate that the inhibition of A β -induced neuronal damage by MRTF-A is related to the rescue of autophagy damage.

Detection and verification of miRNA microarray in A β -treated SH-SY5Y cells

To test the mechanism of MRTF-A on autophagy, transfection of A β -treated SH-SY5Y cells with LV-

MRTF-A or its negative carrier were subjected to miRNA microarray analysis, and normal was as control. As shown in Figure 5A, compared with A β ₁₋₄₂ treatment group, transfection of LV-MRTF-A increased cell viability (Figure 5A). The microarray data that there were 207 differential expressed miRNAs (DEMs). Next, the DEMs underwent venn analysis (Figure 5B, 5C). A total of 8 significantly DEMs were determined, including one up-regulated and seven down-regulated. To confirm the regulatory effect of MRTF-A on miR-1273g-3p, A β -treated SH-SY5Y cells were transfected

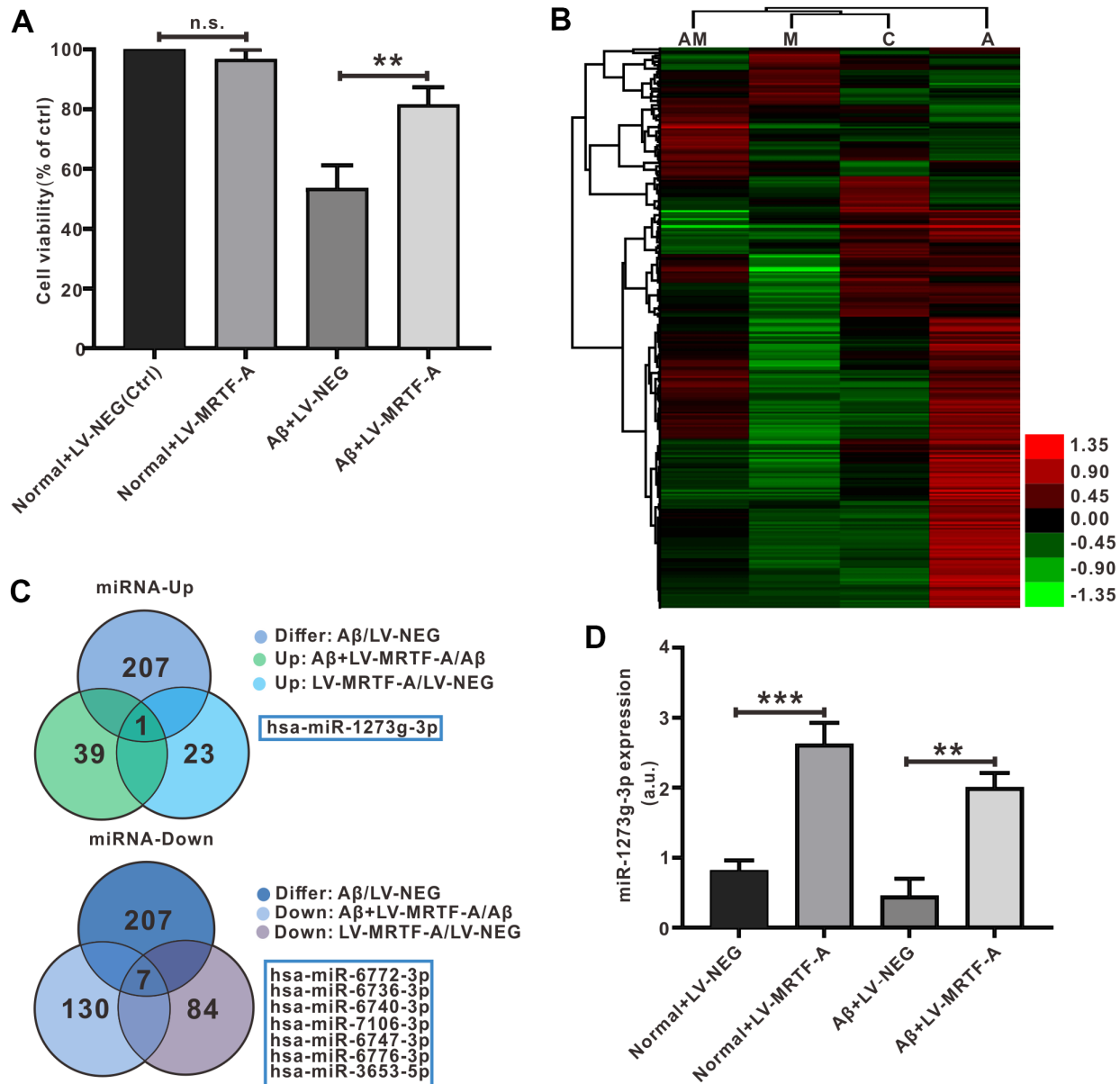


Figure 5. Detection and verification of miRNA microarray in A β -treated SH-SY5Y cells. (A) MRTF-A increased cell viability that had been reduced by A β ₁₋₄₂ exposure (n=6). (B) Microarray cluster analysis (n=3). AM: A β +LV-MRTF-A, M: normal+LV-MRTF-A, C: normal+LV-NEG, A: A β +LV-NEG. (C) Venn plots showed DEMs. (D) The miR-1273g-3p level was analyzed by RT-PCR. Data represent means \pm SEM of 3 independent experiments. * P < 0.05, ** P < 0.01 and *** P < 0.001 (one-way ANOVA, Tukey's Multiple Comparison Test).

with LV-MRTF-A. As shown in Figure 5D, LV-MRTF-A significantly increased miR-1273g-3p level (≥ 4.2 times) in normal or A β -treated SH-SY5Y cells (Figure 5D).

mTOR was the target gene of miR-1273g-3p

In order to explore the mechanism of miR-1273g-3p on A β -induced neuronal damage, miRBase and Targetscan were used to predict the target genes of miR-1273g-3p. We obtained the sequence of miR-1273b-3p and mTOR 3'-UTR through miRbase and found the complementary pairing region between miR-

1273g-3p and mTOR sequence in the 3'-UTR of Homo sapiens (Hsa) (Figure 6A). The analysis of gene function Gene Ontology and Kyoto Encyclopedia of Genes and Genomes database suggested that the binding sites of miR-1273g-3p enriched autophagy genes, and mTOR was one of the most potential target genes (Supplementary Figure 3). Bibiserv2 software was also used to analyze 3'-UTR Hybrid energy analysis between miR-1273g-3p and mTOR. The results showed that the free energy was lower (-46.7 kcal/mol), speculating that both binding sites may have strong binding ability and produce its high efficiency (Supplementary Figure 4).

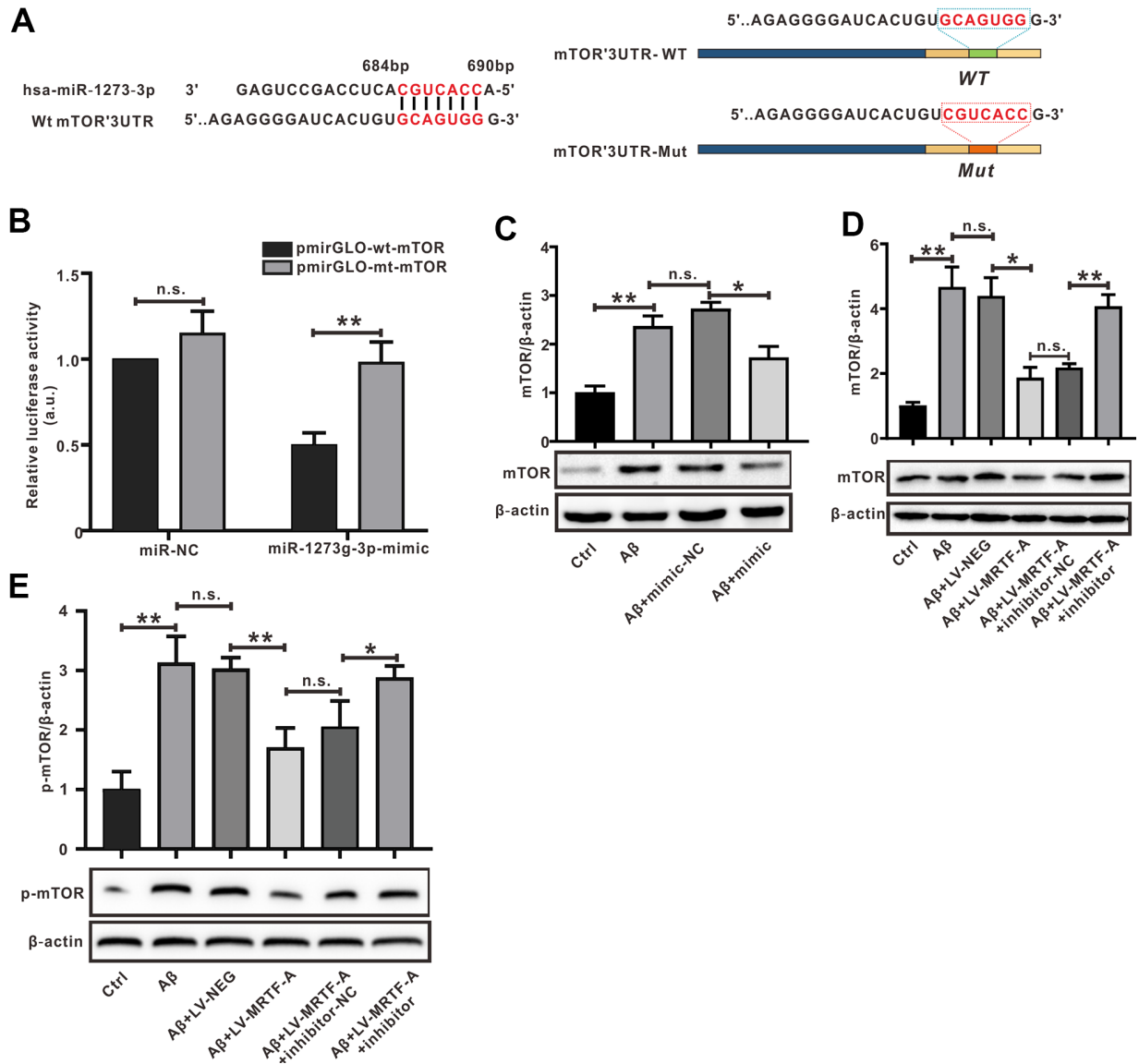


Figure 6. mTOR was the target of miR-1273g-3p. (A) A complementary pairing area or mutant area was shown between miR-1273g-3p and 3'-UTR mTOR with the wild type or mutant type, respectively. (B) The dual luciferase reporter assay. (C-E) The protein expression of mTOR and p-mTOR was detected by western blot. Data represent means \pm SEM of 3 independent experiments. * $P < 0.05$, ** $P < 0.01$ and *** $P < 0.001$ (one-way ANOVA, Tukey's Multiple Comparison Test).

To verify whether mTOR was a target gene of miR-1273g-3p, the dual luciferase reporter assay was performed (Figure 6B). The luciferase activity of mTOR-wt luciferase reporter vector was notably suppressed in response to transduction of miR-1273g-3p mimic when compared with the mimic-NC group ($P < 0.05$), indicating a direct combination between miR-1273g-3p and mTOR 3'-UTR. Western blot analysis confirmed that transduction of miR-1273g-3p mimic in A β -treated SH-SY5Y cells negatively regulated mTOR protein expression by targeting mTOR 3'-UTR (Figure 6C); meanwhile, transfection of LV-MRTF-A decreased the expression of mTOR and its phosphorylated (p-mTOR) proteins; however, this effect was abrogated by co-transfection with miR-1273g-3p inhibitor (Figure 6D, 6E).

miR-1273g-3p/mTOR axis involved in the role of MRTF-A on A β -induced autophagy impairment

To explore the effect of miR-1273g-3p on A β -induced neuronal autophagy impairment. Cells were transfected with miR-1273g-3p mimic or its negative vector for 48 hours and then exposed to A β_{1-42} . 24 hours later, western blotting showed that miR-1273g-3p significantly increased the expression of LC3II and Beclin1 and decreased the level of p62 compared with the A β +mimic-NC group (Figure 7A, 7B). Autophagy flow analysis showed that normal SH-SY5Y cells exhibited basal autophagy; however, the cells subjected to A β_{1-42} exhibited increased autophagosomes and few autolysosomes. Upregulating of miR-1273g-3p significantly increased the formation of autolysosomes compared with that in A β +mimic-NC, but this effect was declined by MHY1485 (an agonist of mTOR) (Figure 7C). These results indicated that miR-1273g-3p reversed A β -induced autophagy impairment partially dependent on mTOR pathway.

To further confirm whether miR-1273g-3p is involved in the activation of autophagy by MRTF-A, the cells were transduced with LV-MRTF-A and co-transfected with or without miR-1273g-3p inhibitor. As expected, compared with the A β or A β +LV-NEG group, transduction of LV-MRTF-A significantly increased the formation of autolysosomes in A β -treated cells, and this effect was partially eliminated by co-treatment with miR-1273g-3p inhibitor (Figure 7C). Western blotting showed that overexpression of MRTF-A increased the expression of LC3II and Beclin1 and decreased p62 levels, which was also partially reversed by miR-1273g-3p inhibitor (Figure 7D, 7E). Accordingly, overexpression of MRTF-A showed a significant inhibitory effect on apoptosis, but in SH-SY5Y cells treated with A β , this effect was partially reversed by co-treatment with miR-1273g-3p inhibitor (Figure 7F, 7G).

DISCUSSION

In the present study, we investigated the effects and the underlying mechanism of MRTF-A on A β -induced neurotoxicity and autophagy dysfunction *in vivo* and *in vitro* Alzheimer models. Our current research shows that there is a decreasing of MRTF-A protein in the hippocampus of Tg2576 mice, which is related to its learning and memory impairment. Overexpression of MRTF-A improved memory impairment and cognitive function in Tg2576 AD mouse model.

Alzheimer's disease is characterized by accumulation of amyloid beta (A β) and tau protein in the brain, leading to neurodegeneration with progressive cognitive decline [41, 42]. Tg2576 mice, as AD experimental models, exhibit A β accumulation and cognitive deficits, and overexpress human amyloid precursor protein (hAPP) subtype 695 containing the Swedish double mutation [31, 32]. In A β -treated cells and animal models, the level of APP and BACE1 is involved in A β production, leading to increased A β -induced neuronal toxicity. We firstly demonstrated that upregulating MRTF-A significantly decreased the A β plaques accumulation and reduced the protein expression of APP and BACE1 and alleviated hippocampal neuronal damage in Tg2576 mice.

Interestingly, the analysis of co-expression network construction revealed that MRTF-A function was related to autophagy related genes such as Beclin1 and ATG5 and so on, suggesting MRTF-A involving in autophagy process. Accumulating evidence showed that the impairment in the autophagy-lysosome system disturbs the turnover of other molecules associated with Alzheimer's disease, which may also contribute to the neuronal dysfunction in Alzheimer's disease [43, 44]. Several lines of evidence have suggested that a tight relationship between A β production and mTOR in AD. Activation of PI3K/Akt/mTOR increased amyloid precursor protein synthesis and deposition, in part by inhibiting autophagy mediated A β clearance, while restoration of autophagy reverses cognitive decline and ameliorated A β pathology [37, 45]. Beclin1 and LC3 initiate autophagogenesis by interacting with ATG3/ATG7 effectors. The P62 protein is an adaptor that binds LC3 on autophagosomes to ubiquitinated proteins on cargo to recruit autophagosomes, which is continuously degraded by autophagy-lysosomal system. Autophagy dysfunction led to p62 accumulation [46]. In the present study, autophagy dysfunction was also found in the hippocampal region of Tg2576 mice, which was partially restored by upregulating MRTF-A, the similar results were confirmed in SH-SY5Y cells after exposed to A β_{1-42} . We found that overexpression of MRTF-A could decreased p62 protein expression and increased Beclin1 protein level both *in vivo* and *in vitro*.

In vitro autophagy flux analysis also showed that MRTF-A can rescue A β -induced autophagy damage, which is the reason for the inhibitory effect of MRTF-A on A β -induced apoptosis of SH-SY5Y cells.

MiRNAs is reported that miRNAs are involved in a variety of human diseases [47], including in the autophagy process following AD. Increasing evidence has shown that miRNAs are strongly associated with

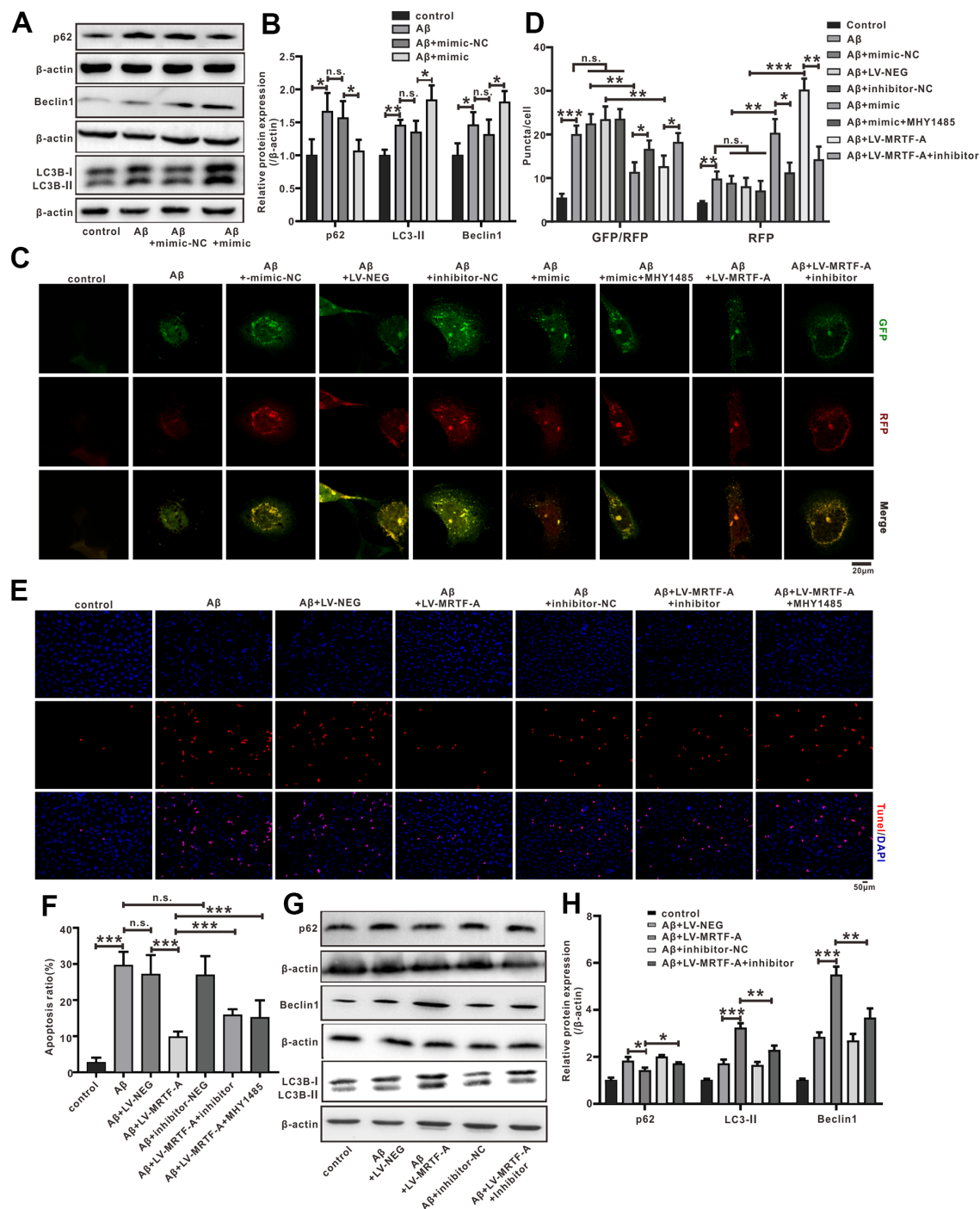


Figure 7. The miR-1273g-3p/mTOR axis involved in MRTF-A against A β -induced autophagy impairment and neuronal apoptosis in SH-SY5Y cells. (A, B) LC3II, Beclin1 and p62 level was upregulated by miR-1273g-3p. (C, D) The autophagy flux analysis using Ad-mCherry-GFP-LC3B-tagged protein. (E, F) TUNEL staining for cell apoptosis. (G, H) LC3II, Beclin1 and p62 level was upregulated by MRTF-A. Data represent means \pm SEM of 3 independent experiments. * P < 0.05, ** P < 0.01 and * P < 0.001 (one-way ANOVA, Tukey's Multiple Comparison Test).**

AD [48]. Because there is some correlation between miRNA and autophagy [49]. We postulated that the effect of MRTF-A on autophagy in the pathological process of AD was associated with miRNAs. For the purpose, we next performed miRNAs expression profile to predict the differential expressed miRNAs (DEMs) which involved in MRTF-A against A β -induced neuronal damage. The miR-1273g-3p was identified as one of the most significant DEMs. Bioinformatics analysis shows that miR-1273g-3p is enriched in autophagy genes, and mTOR is one of the most potential target genes. The mTOR gene, a negative regulator of autophagy, can play the role of “gatekeeper” for autophagy initiation, which plays a central role in autophagy regulation and also the central link of PI3K/AKT signaling pathway [50–53]. Furthermore, the binding free energy between miR-1273g-3p and mTOR was low, speculating the strong binding ability. The results of dual luciferase reporter assay and western blot showed that miR-1273g-3p negative regulated the level of mTOR and p-mTOR protein. The relationship between MRTF-A and miR-1273g-3p/mTOR axis prompted us to speculate that miR-1273g-3p is involved in the effect of MRTF-A on

autophagy. As predicted, the use of miR-1273g-3p alone increased the protein expression of LC3II and Beclin1 and decreased p62 expression of, and at the same time enhanced the autophagy flux, and this effect could be eliminated by MHY1485 (mTOR agonist), indicating that miR-1273g-3p can rescue A β -induced autophagy damage partially depends on the mTOR pathway. In addition, we also found that MRTF-A-mediated recovery of autophagy impairment by promoting miR-1273g-3p/mTOR axis helps protect MRTF-A from neuronal damage.

CONCLUSIONS

Our study shows that MRTF-A improves cognitive deficit of Alzheimer mice and alleviated A β -induced neurotoxicity *in vivo* and *in vitro*. Further, MRTF-A rescues the A β -induced autophagy impairment via regulating miR-1273g-3p/mTOR axis, which maybe contributes to the protective effect of MRTF-A against A β -induced neurotoxicity. Therefore, upregulation of MRTF-A or activation of miR-1273g-3p/mTOR axis may serve as a potential therapeutic target in AD treatment. (Summarized in Figure 8).

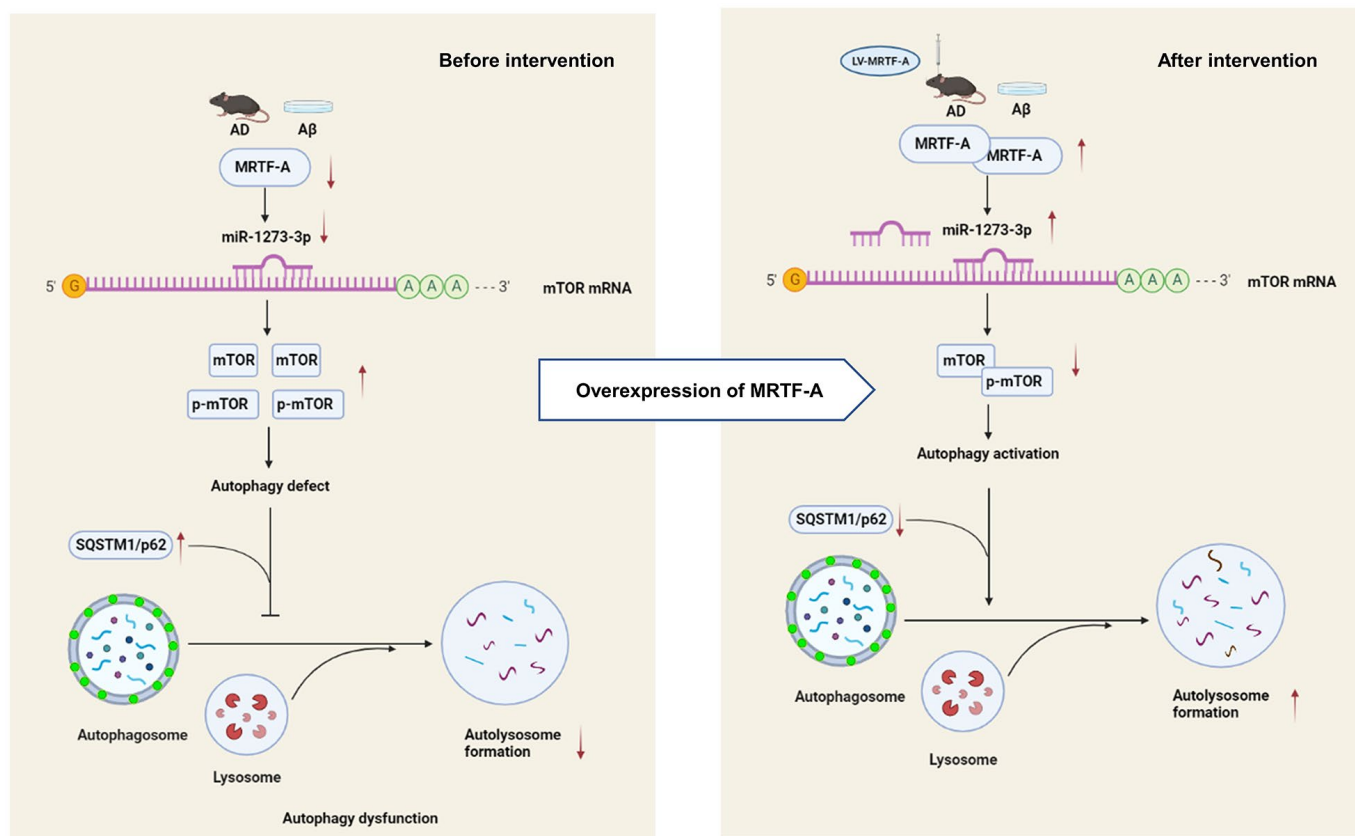


Figure 8. The schematic description of the mechanism of MRTF-A/miR-1273g-3p/mTOR axis in regulating autophagy in Alzheimer models.

Abbreviations

AD: Alzheimer's Disease; AVs: autophagic vacuoles; CNS: Central nervous system; MAP1LC3/LC3: microtubule associated protein1 light chain 3; mTOR: mammalian target of rapamycin; MRTF-A: Myocardin-Related Transcription Factors A; MWM: Morris Water Maze; NFT: neurofibrillary tangles; intracerebroventricularly: i. c. v.; A β : β -amyloid; HRP: corresponding horseradish peroxidase; Hsa: Homo sapiens; LV: lentivirus; miRNAs: microRNAs; ncRNAs: non-coding RNAs; LV-NEG: LV-negative-EGFP; siRNAs: small-interfering RNA; TUNEL: terminal deoxynucleotidyl transferase dUTP nick-end labeling; 3-MA: 3-Methyladenine.

AUTHOR CONTRIBUTIONS

XH and ZJ designed a research plan. WZ and YY organized the experiment and collected data. YY and ZX conducted animal experiments, and ZY and FM conducted *in vitro* studies. JC, WW analyzed the data and performed statistical analysis. LH and YD conducted bioinformatics research. WZ, XH completed the manuscript. All authors read and approved the final manuscript.

CONFLICTS OF INTEREST

The authors declare that they have no conflicts of interest.

FUNDING

This study was partly supported by Hubei Provincial Health Committee Joint Fund (WJ2019H165), Collaborative innovation key project of Shanghai University of Medicine and Health Sciences, Natural Science Foundation of China (31171327) and Hubei Provincial Health and Family Planning Commission Project (WJ2018H0046).

REFERENCES

1. Wang Y, Balaji V, Kaniyappan S, Krüger L, Irsen S, Tepper K, Chandupatla R, Maetzler W, Schneider A, Mandelkow E, Mandelkow EM. The release and trans-synaptic transmission of Tau via exosomes. *Mol Neurodegener.* 2017; 12:5. <https://doi.org/10.1186/s13024-016-0143-y> PMID:[28086931](https://pubmed.ncbi.nlm.nih.gov/28086931/)
2. Do KV, Kautzmann MI, Jun B, Gordon WC, Nshimiyimana R, Yang R, Petasis NA, Bazan NG. Elovans counteract oligomeric β -amyloid-induced gene expression and protect photoreceptors. *Proc Natl Acad Sci USA.* 2019; 116:24317–25. <https://doi.org/10.1073/pnas.1912959116> PMID:[31712409](https://pubmed.ncbi.nlm.nih.gov/31712409/)
3. Rad SK, Arya A, Karimian H, Madhavan P, Rizwan F, Koshy S, Prabhu G. Mechanism involved in insulin resistance via accumulation of β -amyloid and neurofibrillary tangles: link between type 2 diabetes and Alzheimer's disease. *Drug Des Devel Ther.* 2018; 12:3999–4021. <https://doi.org/10.2147/DDDT.S173970> PMID:[30538427](https://pubmed.ncbi.nlm.nih.gov/30538427/)
4. Sölvander S, Nikitidou E, Brolin R, Söderberg L, Sehlin D, Lannfelt L, Erlandsson A. Accumulation of amyloid- β by astrocytes result in enlarged endosomes and microvesicle-induced apoptosis of neurons. *Mol Neurodegener.* 2016; 11:38. <https://doi.org/10.1186/s13024-016-0098-z> PMID:[27176225](https://pubmed.ncbi.nlm.nih.gov/27176225/)
5. Wegiel J, Frackowiak J, Mazur-Kolecka B, Schanen NC, Cook EH Jr, Sigman M, Brown WT, Kuchna I, Wegiel J, Nowicki K, Imaki H, Ma SY, Chauhan A, et al. Abnormal intracellular accumulation and extracellular A β deposition in idiopathic and Dup15q11.2-q13 autism spectrum disorders. *PLoS One.* 2012; 7:e35414. <https://doi.org/10.1371/journal.pone.0035414> PMID:[22567102](https://pubmed.ncbi.nlm.nih.gov/22567102/)
6. Gontier G, George C, Chaker Z, Holzenberger M, Aïd S. Blocking IGF Signaling in Adult Neurons Alleviates Alzheimer's Disease Pathology through Amyloid- β Clearance. *J Neurosci.* 2015; 35:11500–13. <https://doi.org/10.1523/JNEUROSCI.0343-15.2015> PMID:[26290229](https://pubmed.ncbi.nlm.nih.gov/26290229/)
7. Yu WH, Cuervo AM, Kumar A, Peterhoff CM, Schmidt SD, Lee JH, Mohan PS, Mercken M, Farmery MR, Tjernberg LO, Jiang Y, Duff K, Uchiyama Y, et al. Macroautophagy—a novel Beta-amyloid peptide-generating pathway activated in Alzheimer's disease. *J Cell Biol.* 2005; 171:87–98. <https://doi.org/10.1083/jcb.200505082> PMID:[16203860](https://pubmed.ncbi.nlm.nih.gov/16203860/)
8. Parmacek MS. Myocardin-related transcription factors: critical coactivators regulating cardiovascular development and adaptation. *Circ Res.* 2007; 100:633–44. <https://doi.org/10.1161/01.RES.0000259563.61091.e8> PMID:[17363709](https://pubmed.ncbi.nlm.nih.gov/17363709/)
9. Alberti S, Krause SM, Kretz O, Philippar U, Lemberger T, Casanova E, Wiebel FF, Schwarz H, Frotscher M, Schütz G, Nordheim A. Neuronal migration in the murine rostral migratory stream requires serum response factor. *Proc Natl Acad Sci USA.* 2005; 102:6148–53. <https://doi.org/10.1073/pnas.0501191102> PMID:[15837932](https://pubmed.ncbi.nlm.nih.gov/15837932/)

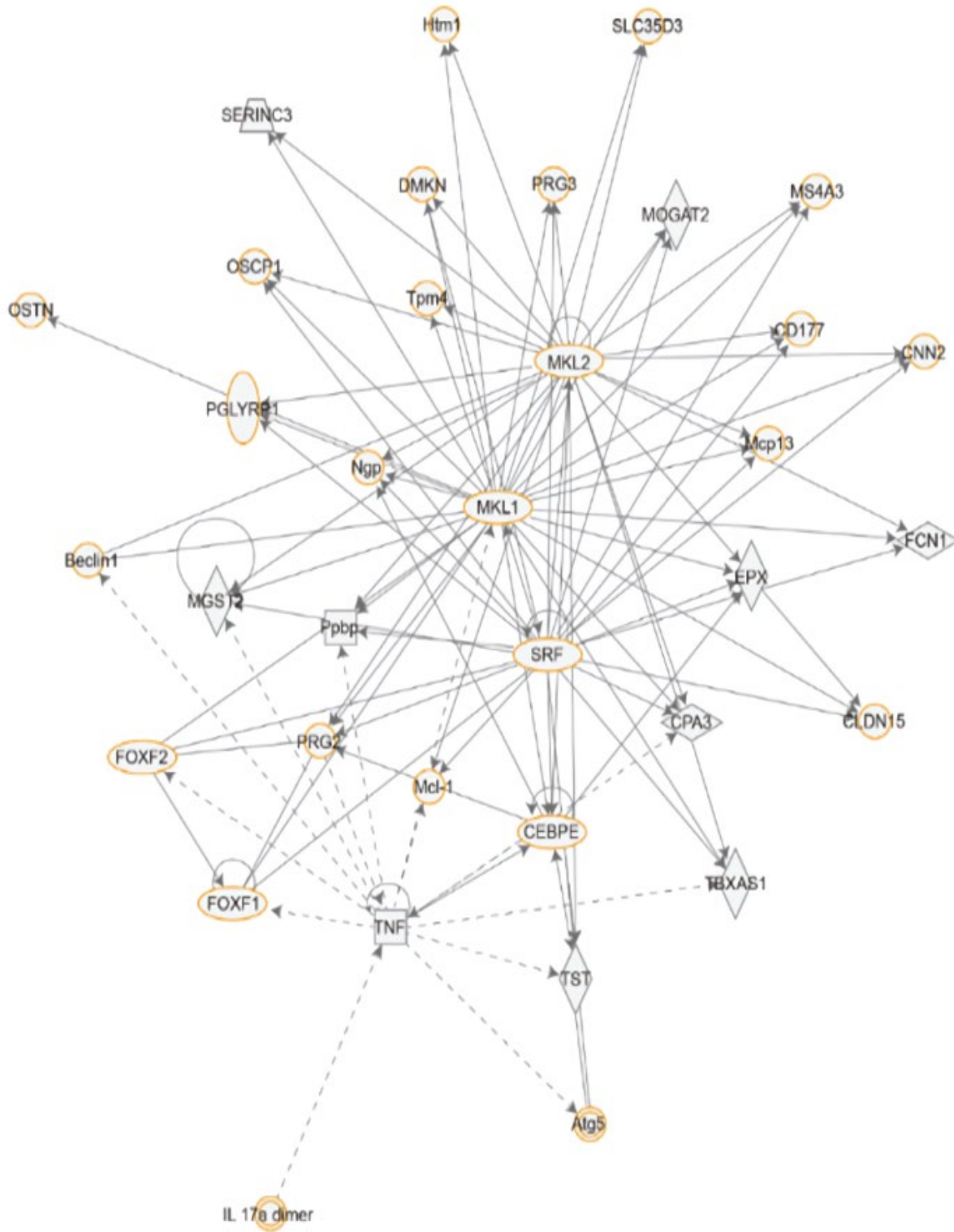
10. Shiota J, Ishikawa M, Sakagami H, Tsuda M, Baraban JM, Tabuchi A. Developmental expression of the SRF co-activator MAL in brain: role in regulating dendritic morphology. *J Neurochem*. 2006; 98:1778–88. <https://doi.org/10.1111/j.1471-4159.2006.03992.x> PMID:[16945101](https://pubmed.ncbi.nlm.nih.gov/16945101/)
11. Mokalled MH, Johnson A, Kim Y, Oh J, Olson EN. Myocardin-related transcription factors regulate the Cdk5/Pctaire1 kinase cascade to control neurite outgrowth, neuronal migration and brain development. *Development*. 2010; 137:2365–74. <https://doi.org/10.1242/dev.047605> PMID:[20534669](https://pubmed.ncbi.nlm.nih.gov/20534669/)
12. Zheng WX, Cao XL, Wang F, Wang J, Ying TZ, Xiao W, Zhang Y, Xing H, Dong W, Xu SQ, Min ZL, Wu FJ, Hu XM. Baicalin inhibiting cerebral ischemia/hypoxia-induced neuronal apoptosis via MRTF-A-mediated transactivity. *Eur J Pharmacol*. 2015; 767:201–10. <https://doi.org/10.1016/j.ejphar.2015.10.027> PMID:[26485504](https://pubmed.ncbi.nlm.nih.gov/26485504/)
13. Zhang Y, Pan HY, Hu XM, Cao XL, Wang J, Min ZL, Xu SQ, Xiao W, Yuan Q, Li N, Cheng J, Zhao SQ, Hong X. The role of myocardin-related transcription factor-A in A β 25–35 induced neuron apoptosis and synapse injury. *Brain Res*. 2016; 1648:27–34. <https://doi.org/10.1016/j.brainres.2016.07.003> PMID:[27387387](https://pubmed.ncbi.nlm.nih.gov/27387387/)
14. Lukiw WJ, Alexandrov PN. Regulation of complement factor H (CFH) by multiple miRNAs in Alzheimer's disease (AD) brain. *Mol Neurobiol*. 2012; 46:11–9. <https://doi.org/10.1007/s12035-012-8234-4> PMID:[22302353](https://pubmed.ncbi.nlm.nih.gov/22302353/)
15. Eichhorn SW, Guo H, McGeary SE, Rodriguez-Mias RA, Shin C, Baek D, Hsu SH, Ghoshal K, Villén J, Bartel DP. mRNA destabilization is the dominant effect of mammalian microRNAs by the time substantial repression ensues. *Mol Cell*. 2014; 56:104–15. <https://doi.org/10.1016/j.molcel.2014.08.028> PMID:[25263593](https://pubmed.ncbi.nlm.nih.gov/25263593/)
16. Ma N, Tie C, Yu B, Zhang W, Wan J. Identifying lncRNA-miRNA-mRNA networks to investigate Alzheimer's disease pathogenesis and therapy strategy. *Aging (Albany NY)*. 2020; 12:2897–920. <https://doi.org/10.18632/aging.102785> PMID:[32035423](https://pubmed.ncbi.nlm.nih.gov/32035423/)
17. Saxton RA, Sabatini DM. mTOR Signaling in Growth, Metabolism, and Disease. *Cell*. 2017; 168:960–76. <https://doi.org/10.1016/j.cell.2017.02.004> PMID:[28283069](https://pubmed.ncbi.nlm.nih.gov/28283069/)
18. Williams A, Sarkar S, Cuddon P, Ttofi EK, Saiki S, Siddiqi FH, Jahreiss L, Fleming A, Pask D, Goldsmith P, O'Kane CJ, Floto RA, Rubinsztein DC. Novel targets for Huntington's disease in an mTOR-independent autophagy pathway. *Nat Chem Biol*. 2008; 4:295–305. <https://doi.org/10.1038/nchembio.79> PMID:[18391949](https://pubmed.ncbi.nlm.nih.gov/18391949/)
19. Salama RM, Abdel-Latif GA, Abbas SS, El Magdoub HM, Schaaln MF. Neuroprotective effect of crocin against rotenone-induced Parkinson's disease in rats: Interplay between PI3K/Akt/mTOR signaling pathway and enhanced expression of miRNA-7 and miRNA-221. *Neuropharmacology*. 2020; 164:107900. <https://doi.org/10.1016/j.neuropharm.2019.107900> PMID:[31811872](https://pubmed.ncbi.nlm.nih.gov/31811872/)
20. Li C, Chen Y, Chen X, Wei Q, Cao B, Shang H. Downregulation of MicroRNA-193b-3p Promotes Autophagy and Cell Survival by Targeting TSC1/mTOR Signaling in NSC-34 Cells. *Front Mol Neurosci*. 2017; 10:160. <https://doi.org/10.3389/fnmol.2017.00160> PMID:[28611587](https://pubmed.ncbi.nlm.nih.gov/28611587/)
21. Balgi AD, Fonseca BD, Donohue E, Tsang TC, Lajoie P, Proud CG, Nabi IR, Roberge M. Screen for chemical modulators of autophagy reveals novel therapeutic inhibitors of mTORC1 signaling. *PLoS One*. 2009; 4:e7124. <https://doi.org/10.1371/journal.pone.0007124> PMID:[19771169](https://pubmed.ncbi.nlm.nih.gov/19771169/)
22. Chen H, Chen F, Zhang M, Chen Y, Cui L, Liang C. A Review of APOE Genotype-Dependent Autophagic Flux Regulation in Alzheimer's Disease. *J Alzheimers Dis*. 2021; 84:535–55. <https://doi.org/10.3233/JAD-210602> PMID:[34569952](https://pubmed.ncbi.nlm.nih.gov/34569952/)
23. Ng CT, Jaworski JP, Jayaraman P, Sutton WF, Delio P, Kuller L, Anderson D, Landucci G, Richardson BA, Burton DR, Forthal DN, Haigwood NL. Passive neutralizing antibody controls SHIV viremia and enhances B cell responses in infant macaques. *Nat Med*. 2010; 16:1117–9. <https://doi.org/10.1038/nm.2233> PMID:[20890292](https://pubmed.ncbi.nlm.nih.gov/20890292/)
24. Bonow RH, Aïd S, Zhang Y, Becker KG, Bosetti F. The brain expression of genes involved in inflammatory response, the ribosome, and learning and memory is altered by centrally injected lipopolysaccharide in mice. *Pharmacogenomics J*. 2009; 9:116–26. <https://doi.org/10.1038/tpj.2008.15> PMID:[18957951](https://pubmed.ncbi.nlm.nih.gov/18957951/)
25. Zhang R, Zhou W, Yu Z, Yang L, Liu G, Yu H, Zhou Q, Min Z, Zhang C, Wu Q, Hu XM, Yuan Q. miR-1247-3p mediates apoptosis of cerebral neurons by targeting caspase-2 in stroke. *Brain Res*. 2019; 1714:18–26. <https://doi.org/10.1016/j.brainres.2019.02.020> PMID:[30779911](https://pubmed.ncbi.nlm.nih.gov/30779911/)
26. Ham HJ, Han SB, Yun J, Yeo IJ, Ham YW, Kim SH, Park PH, Choi DY, Hong JT. Bee venom phospholipase A2 ameliorates amyloidogenesis and neuroinflammation through inhibition of signal transducer and activator of

- transcription-3 pathway in Tg2576 mice. *Transl Neurodegener.* 2019; 8:26.
<https://doi.org/10.1186/s40035-019-0167-7>
PMID:[31592103](https://pubmed.ncbi.nlm.nih.gov/31592103/)
27. Morris R. Developments of a water-maze procedure for studying spatial learning in the rat. *J Neurosci Methods.* 1984; 11:47–60.
[https://doi.org/10.1016/0165-0270\(84\)90007-4](https://doi.org/10.1016/0165-0270(84)90007-4)
PMID:[6471907](https://pubmed.ncbi.nlm.nih.gov/6471907/)
28. Hu X, Xiang Z, Zhang W, Yu Z, Xin X, Zhang R, Deng Y, Yuan Q. Protective effect of DLX6-AS1 silencing against cerebral ischemia/reperfusion induced impairments. *Aging (Albany NY).* 2020; 12:23096–113.
<https://doi.org/10.18632/aging.104070>
PMID:[33216728](https://pubmed.ncbi.nlm.nih.gov/33216728/)
29. Han H, Sun D, Li W, Shen H, Zhu Y, Li C, Chen Y, Lu L, Li W, Zhang J, Tian Y, Li Y. A c-Myc-MicroRNA functional feedback loop affects hepatocarcinogenesis. *Hepatology.* 2013; 57:2378–89.
<https://doi.org/10.1002/hep.26302>
PMID:[23389829](https://pubmed.ncbi.nlm.nih.gov/23389829/)
30. Xiao Y, Zhou Y, Lu Y, Zhou K, Cai W. PHB2 interacts with LC3 and SQSTM1 is required for bile acids-induced mitophagy in cholestatic liver. *Cell Death Dis.* 2018; 9:160.
<https://doi.org/10.1038/s41419-017-0228-8>
PMID:[29416008](https://pubmed.ncbi.nlm.nih.gov/29416008/)
31. Hsiao K, Chapman P, Nilsen S, Eckman C, Harigaya Y, Younkin S, Yang F, Cole G. Correlative memory deficits, Abeta elevation, and amyloid plaques in transgenic mice. *Science.* 1996; 274:99–102.
<https://doi.org/10.1126/science.274.5284.99>
PMID:[8810256](https://pubmed.ncbi.nlm.nih.gov/8810256/)
32. Westerman MA, Cooper-Blacketer D, Mariash A, Kotilinek L, Kawarabayashi T, Younkin LH, Carlson GA, Younkin SG, Ashe KH. The relationship between Abeta and memory in the Tg2576 mouse model of Alzheimer's disease. *J Neurosci.* 2002; 22:1858–67.
<https://doi.org/10.1523/JNEUROSCI.22-05-01858.2002>
PMID:[11880515](https://pubmed.ncbi.nlm.nih.gov/11880515/)
33. Kawarabayashi T, Younkin LH, Saido TC, Shoji M, Ashe KH, Younkin SG. Age-dependent changes in brain, CSF, and plasma amyloid (beta) protein in the Tg2576 transgenic mouse model of Alzheimer's disease. *J Neurosci.* 2001; 21:372–81.
<https://doi.org/10.1523/JNEUROSCI.21-02-00372.2001>
PMID:[11160418](https://pubmed.ncbi.nlm.nih.gov/11160418/)
34. Funderburk SF, Marcellino BK, Yue Z. Cell “self-eating” (autophagy) mechanism in Alzheimer's disease. *Mt Sinai J Med.* 2010; 77:59–68.
<https://doi.org/10.1002/msj.20161>
PMID:[20101724](https://pubmed.ncbi.nlm.nih.gov/20101724/)
35. Carroll B, Korolchuk VI, Sarkar S. Amino acids and autophagy: cross-talk and co-operation to control cellular homeostasis. *Amino Acids.* 2015; 47:2065–88.
<https://doi.org/10.1007/s00726-014-1775-2>
PMID:[24965527](https://pubmed.ncbi.nlm.nih.gov/24965527/)
36. Komatsu M, Waguri S, Chiba T, Murata S, Iwata J, Tanida I, Ueno T, Koike M, Uchiyama Y, Kominami E, Tanaka K. Loss of autophagy in the central nervous system causes neurodegeneration in mice. *Nature.* 2006; 441:880–4.
<https://doi.org/10.1038/nature04723> PMID:[16625205](https://pubmed.ncbi.nlm.nih.gov/16625205/)
37. Zhang Z, Wang X, Zhang D, Liu Y, Li L. Geniposide-mediated protection against amyloid deposition and behavioral impairment correlates with downregulation of mTOR signaling and enhanced autophagy in a mouse model of Alzheimer's disease. *Aging (Albany NY).* 2019; 11:536–48.
<https://doi.org/10.18632/aging.101759>
PMID:[30684442](https://pubmed.ncbi.nlm.nih.gov/30684442/)
38. Bergamini E. Autophagy: a cell repair mechanism that retards ageing and age-associated diseases and can be intensified pharmacologically. *Mol Aspects Med.* 2006; 27:403–10.
<https://doi.org/10.1016/j.mam.2006.08.001>
PMID:[16973211](https://pubmed.ncbi.nlm.nih.gov/16973211/)
39. Dooley HC, Razi M, Polson HE, Girardin SE, Wilson MI, Tooze SA. WIPI2 links LC3 conjugation with PI3P, autophagosome formation, and pathogen clearance by recruiting Atg12-5-16L1. *Mol Cell.* 2014; 55:238–52.
<https://doi.org/10.1016/j.molcel.2014.05.021>
PMID:[24954904](https://pubmed.ncbi.nlm.nih.gov/24954904/)
40. Xu Y, Zhang J, Tian C, Ren K, Yan YE, Wang K, Wang H, Chen C, Wang J, Shi Q, Dong XP. Overexpression of p62/SQSTM1 promotes the degradations of abnormally accumulated PrP mutants in cytoplasm and relieves the associated cytotoxicities via autophagy-lysosome-dependent way. *Med Microbiol Immunol.* 2014; 203:73–84.
<https://doi.org/10.1007/s00430-013-0316-z>
PMID:[24240628](https://pubmed.ncbi.nlm.nih.gov/24240628/)
41. Singh R, Cuervo AM. Autophagy in the cellular energetic balance. *Cell Metab.* 2011; 13:495–504.
<https://doi.org/10.1016/j.cmet.2011.04.004>
PMID:[21531332](https://pubmed.ncbi.nlm.nih.gov/21531332/)
42. Thran J, Poeck B, Strauss R. Serum response factor-mediated gene regulation in a *Drosophila* visual working memory. *Curr Biol.* 2013; 23:1756–63.
<https://doi.org/10.1016/j.cub.2013.07.034>
PMID:[24012317](https://pubmed.ncbi.nlm.nih.gov/24012317/)
43. Nixon RA, Yang DS. Autophagy failure in Alzheimer's disease—locating the primary defect. *Neurobiol Dis.* 2011; 43:38–45.

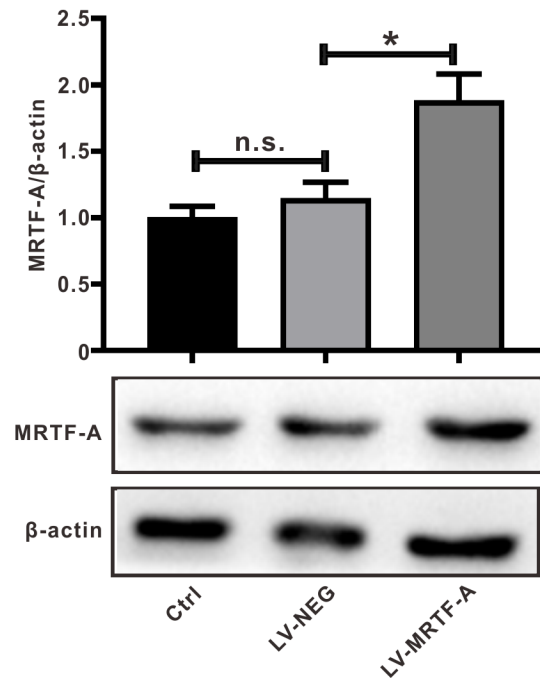
- <https://doi.org/10.1016/j.nbd.2011.01.021>
PMID:[21296668](https://pubmed.ncbi.nlm.nih.gov/21296668/)
44. Kuma A, Komatsu M, Mizushima N. Autophagy-monitoring and autophagy-deficient mice. *Autophagy*. 2017; 13:1619–28.
<https://doi.org/10.1080/15548627.2017.1343770>
PMID:[28820286](https://pubmed.ncbi.nlm.nih.gov/28820286/)
45. Caccamo A, Magri A, Medina DX, Wisely EV, López-Aranda MF, Silva AJ, Oddo S. mTOR regulates tau phosphorylation and degradation: implications for Alzheimer's disease and other tauopathies. *Aging Cell*. 2013; 12:370–80.
<https://doi.org/10.1111/accel.12057>
PMID:[23425014](https://pubmed.ncbi.nlm.nih.gov/23425014/)
46. Lipinski MM, Zheng B, Lu T, Yan Z, Py BF, Ng A, Xavier RJ, Li C, Yankner BA, Scherzer CR, Yuan J. Genome-wide analysis reveals mechanisms modulating autophagy in normal brain aging and in Alzheimer's disease. *Proc Natl Acad Sci USA*. 2010; 107:14164–9.
<https://doi.org/10.1073/pnas.1009485107>
PMID:[20660724](https://pubmed.ncbi.nlm.nih.gov/20660724/)
47. Zhang X, Wang Q, Wang X, Chen X, Shao M, Zhang Q, Guo D, Wu Y, Li C, Wang W, Wang Y. Tanshinone IIA protects against heart failure post-myocardial infarction via AMPKs/mTOR-dependent autophagy pathway. *Biomed Pharmacother*. 2019; 112:108599.
<https://doi.org/10.1016/j.biopha.2019.108599>
PMID:[30798134](https://pubmed.ncbi.nlm.nih.gov/30798134/)
48. Si L, Xu L, Yin L, Qi Y, Han X, Xu Y, Zhao Y, Liu K, Peng J. Potent effects of dioscin against pancreatic cancer via miR-149-3P-mediated inhibition of the Akt1 signalling pathway. *Br J Pharmacol*. 2017; 174:553–68.
<https://doi.org/10.1111/bph.13718> PMID:[28095588](https://pubmed.ncbi.nlm.nih.gov/28095588/)
49. Femminella GD, Ferrara N, Rengo G. The emerging role of microRNAs in Alzheimer's disease. *Front Physiol*. 2015; 6:40.
<https://doi.org/10.3389/fphys.2015.00040>
PMID:[25729367](https://pubmed.ncbi.nlm.nih.gov/25729367/)
50. Zhang Y, Liu C, Wang J, Li Q, Ping H, Gao S, Wang P. MiR-299-5p regulates apoptosis through autophagy in neurons and ameliorates cognitive capacity in APP^{swe}/PS1^{dE9} mice. *Sci Rep*. 2016; 6:24566.
<https://doi.org/10.1038/srep24566> PMID:[27080144](https://pubmed.ncbi.nlm.nih.gov/27080144/)
51. Switon K, Kotulska K, Janusz-Kaminska A, Zmorzynska J, Jaworski J. Molecular neurobiology of mTOR. *Neuroscience*. 2017; 341:112–53.
<https://doi.org/10.1016/j.neuroscience.2016.11.017>
PMID:[27889578](https://pubmed.ncbi.nlm.nih.gov/27889578/)
52. Kim YC, Guan KL. mTOR: a pharmacologic target for autophagy regulation. *J Clin Invest*. 2015; 125:25–32.
<https://doi.org/10.1172/JCI73939> PMID:[25654547](https://pubmed.ncbi.nlm.nih.gov/25654547/)
53. LiCausi F, Hartman NW. Role of mTOR Complexes in Neurogenesis. *Int J Mol Sci*. 2018; 19:1544.
<https://doi.org/10.3390/ijms19051544>
PMID:[29789464](https://pubmed.ncbi.nlm.nih.gov/29789464/)

SUPPLEMENTARY MATERIALS

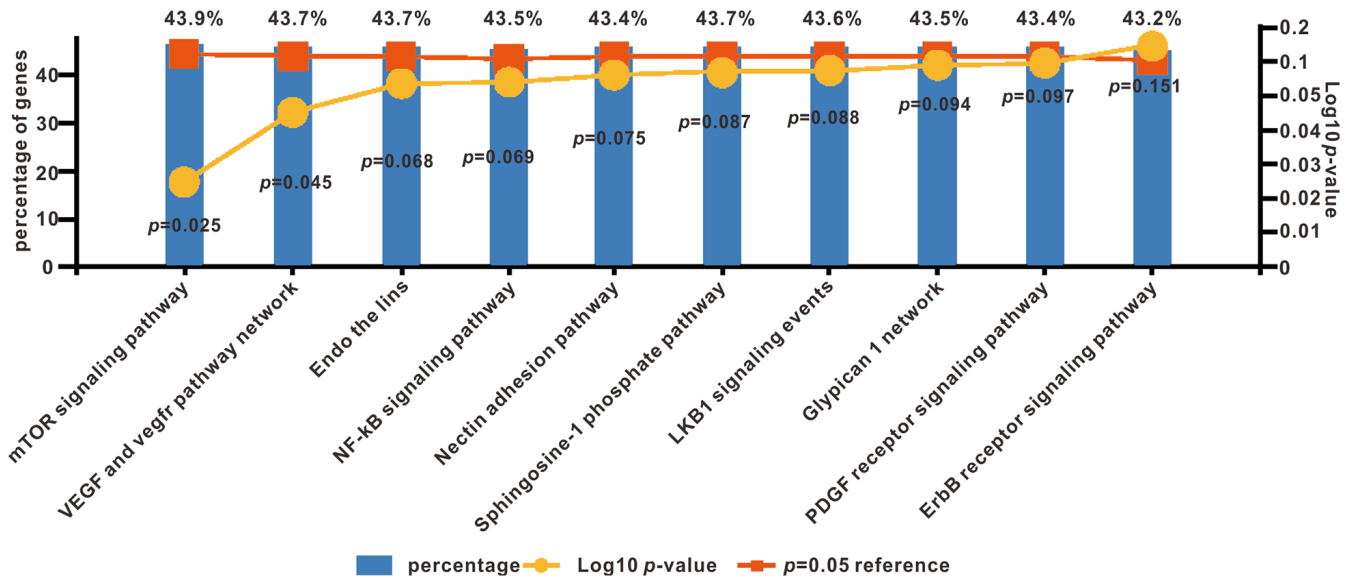
Supplementary Figures



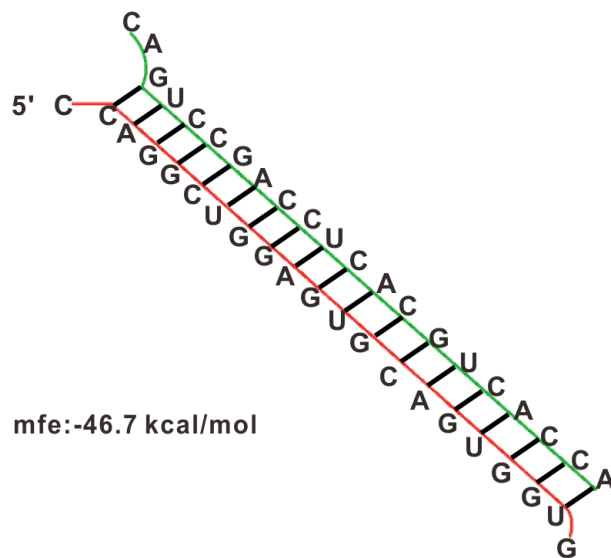
Supplementary Figure 1. The functional and high connected hubs varied about MRTF-A analyzed by IPA tool.



Supplementary Figure 2. MRTF-A protein expression was determined by western blot after transduction with LV-MRTF-A or LV-NEG for 48 hours in SH-SY5Y cells. * $p < 0.05$, ** $p < 0.01$ and *** $p < 0.001$ (one-way ANOVA, Tukey's Multiple Comparison Test).



Supplementary Figure 3. The gene function Gene Ontology (GO) analysis and Kyoto Encyclopedia of Genes and Genomes (KEGG) database analysis to identify the involved enriched pathways.



Supplementary Figure 4. Bibiserv2 software was used to analyze 3'-UTR Hybrid energy analysis between miR-1273g-3p and mTOR.